

# ALMA Memo 371

## Receiver Calibration Schemes for ALMA

S.Guilloteau (IRAM / ESO), R.Moreno (IRAM Grenoble)

June 1, 2001

### Abstract

We re-investigate the two receiver calibration schemes which have been proposed for ALMA: dual loads located in the sub-reflector, or semi transparent vane in front of the receiver. We show that the dual-load system needs to switch with a cycle time of less than 0.1 second to be efficient in the submillimeter regime. Moreover, integrations in excess of 20 seconds are required to get sufficient calibration accuracy at these frequencies. The semi-transparent vane must have an absorption coefficient of only 0.06–0.10 below 100 GHz, but is no longer required at frequencies above 300 GHz. The vane transmission can be calibrated in 2-3 minutes by measurement of an astronomical source (nearby quasar). Two vanes, with absorption coefficient 0.06 and 0.12 respectively, are recommended to minimize the calibration time. Given the simplicity of the vane system (passive, slow device, in the receiver cabin), compared with the complexity, speed and location of the dual-load system, we strongly recommend that ALMA develops and adopts such a scheme for the receiver calibration.

## 1 Basic System Noise

The typical system temperature is derived from the agreed ALMA specifications. We assume the standard ALMA numbers:

$$T_{\text{rec}}(\nu) = 6h\nu/k + 4 \text{ K} \quad (\nu < 400\text{GHz}) \quad \text{and} \quad T_{\text{rec}}(\nu) = 10h\nu/k + 4 \text{ K} \quad (\nu > 400\text{GHz})$$

for single sideband receivers (rejection better than 10 dB).

$$T_{\text{rec}}(\nu) = 3h\nu/k \text{ K} \quad (\nu < 400\text{GHz}) \quad \text{and} \quad T_{\text{rec}}(\nu) = 5h\nu/k \text{ K} \quad (\nu > 400\text{GHz})$$

for double sideband receivers. We also assume the forward efficiency is falling down from 0.95 at low frequencies to 0.90 at 900 GHz (as  $\nu^2$ ).

The atmospheric conditions are taken from the weather statistics percentiles, with temperature adjusted to account (to first order) for the imperfect correlation between temperature and opacity. We assume dynamic scheduling will match the observed frequency to the appropriate observing conditions, more precisely that observations above 370 GHz will be done only in the 25 % best observing time, observations between 270 and 370 GHz only in the 50 % best observing time, and “low” frequency observations in the remaining available good weather (see Table 1). Figure 1 gives the corresponding expected system temperature **in the receiver calibration plane, i.e.**

$$T_{\text{ant}} = T_{\text{rec}} + J_{\text{sky}} \tag{1}$$

(see Eq.4 for the complete expression of  $J_{\text{sky}}$ ).  $T_{\text{ant}}$  is the relevant quantity to compare with load temperatures (rather than the more usual system temperature outside the atmosphere, which is only relevant for the astronomical sources).

Percentile	$\tau(225 \text{ GHz})$	Water vapor		Temperature	Observing Frequency
		Max.	Typical		
75 %	0.117	< 2.3 mm	2.3 mm	+3°C	< 250 GHz
50 %	0.061	< 1.2 mm	1.0 mm	0°C	< 370 GHz
25 %	0.037	< 0.7 mm	0.5 mm	-5°C	700 GHz

Table 1: Adopted percentiles for the computation of the system temperatures. Note that this differs from individual percentiles by trying (grossly) to account for correlations between opacity and temperature.

## 2 Basic Equations

### 2.1 Standard Chopper / Vane Calibration

The calibration can be derived from the output powers measured by the receiver on the sky  $P_{\text{sky}}$  and when looking at a load  $P_{\text{load}}$ , compared to the correlated signal measured by the correlator,  $C_{\text{source}}$ :

$$\begin{aligned}
P_{\text{sky}} &= K(T)(T_{\text{rec}} + J_{\text{sky}}) \\
P_{\text{load}} &= K(T)(T_{\text{rec}} + fJ_{\text{load}} + (1-f)J_{\text{sky}}) \\
C_{\text{source}} &= K(T)g_s\eta e^{-\tau}T_A
\end{aligned} \tag{2}$$

The coefficient  $K(T)$  incorporates possible non linearity of the detector (receiver + amplifiers + backend).  $f$  is the fraction of the beam filled by the load, and  $\eta$  the forward efficiency.  $g_s$  and  $g_i$  are the normalized signal and image gain of the receivers  $g_s + g_i = 1$ . Note that, in terms of image to signal gain ratio,  $g$ ,

$$g_s = 1/(1+g) \quad \text{and} \quad g_i = g/(1+g) \tag{3}$$

The sky emissivity  $J_{\text{sky}}$  is given by

$$\begin{aligned}
J_{\text{sky}} &= g_s(\eta J_{\text{m}}^s(1 - e^{-\tau_s}) + \eta J_{\text{bg}}^s e^{-\tau_s} + (1-\eta)J_{\text{spill}}^s) \\
&\quad + g_i(\eta J_{\text{m}}^i(1 - e^{-\tau_i}) + \eta J_{\text{bg}}^i e^{-\tau_i} + (1-\eta)J_{\text{spill}}^i)
\end{aligned} \tag{4}$$

where  $\tau_j$  is the sky opacity (at the current elevation) and

$$J_{\text{x}}^j = \frac{h\nu_j}{k} \frac{1}{e^{h\nu_j/kT_{\text{x}}} - 1} \tag{5}$$

is the Rayleigh-Jeans equivalent temperature of a black body at  $T_{\text{x}}$  at frequency  $\nu_j$ .  $j$  takes values  $s$  or  $i$  for signal or image bands respectively.  $J_{\text{m}}$  is the effective atmospheric brightness temperature,  $J_{\text{bg}}$  the cosmic background, and  $J_{\text{spill}}$  the spillover. Similarly, the effective load temperature  $J_{\text{load}}$  is

$$J_{\text{load}} = g_s J_{\text{load}}^s + g_i J_{\text{load}}^i \tag{6}$$

A major limitation of the calibration accuracy is the possible saturation of the receiver when looking at a warm load. From [Plambeck memo 321], the saturation curve can be expressed as

$$K(P) = \frac{K_0}{1 + P_{\text{ant}}/P_{\text{sat}}} \tag{7}$$

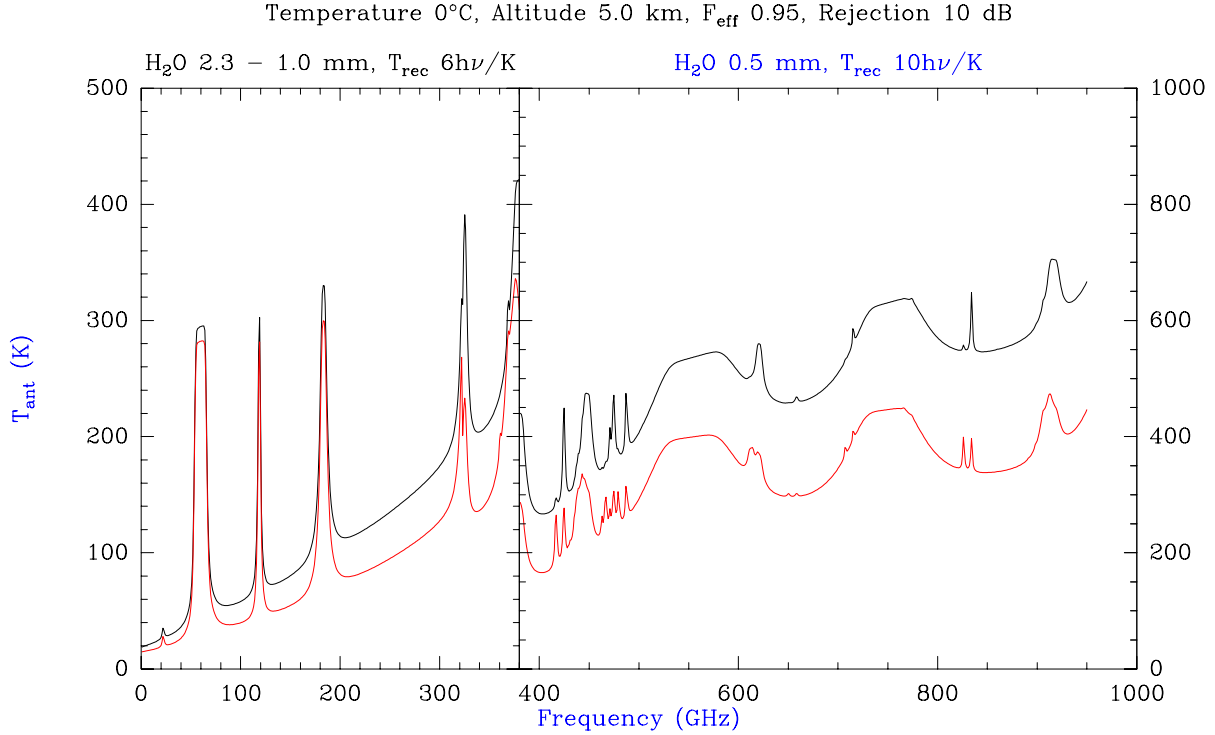


Figure 1: Expected typical antenna plane system temperatures with ALMA. The black curves correspond to Single Side Band tuned receivers (image rejection 10 dB), while the red curves correspond to Double Side Band tuned receivers. Created by `default_tant.astro`

where, for SIS receivers, the saturation power  $P_{\text{sat}}$  is given by

$$P_{\text{sat}} \propto \left( \frac{Nh\nu}{e} \right)^2 \frac{L}{2R} \quad (8)$$

where  $N$  is the number of SIS junctions,  $L$  the mixer conversion loss, and  $R$  the intermediate frequency impedance. The proportionality factor is not known... [Tucker & Feldman 1985]. In terms of noise equivalent temperatures,  $T_{\text{sat}} = P_{\text{sat}} / (k\Delta\nu)$ , where  $\Delta\nu$  is the bandwidth, which shows that, even if saturation was not an issue with current, relatively narrow band (1 GHz), receivers, it may become a limitation for ALMA receivers with 8 GHz bandwidth. We then re-express Eq.7 as

$$K(T) = \frac{K_0}{1 + (T_{\text{ant}}/T_{\text{sat}})} \quad (9)$$

Two strategies have been proposed to minimize this non linearity problem: the dual-load calibration in the subreflector [Bock et al. memo 225], or the semi-transparent vane [Plambeck memo 321]. A similar system was actually used on the IRAM Plateau de Bure antennas: the warm load could be inserted so as to cover partially the beam of the receiver. This particular system was not extremely accurate because of the asymmetric blockage of the aperture. An homogeneous semi-transparent vane covering the whole beam is much preferable.

### 3 Subreflector dual-load system

Instead of having a load covering the full receiver beam, one can have a load in the subreflector which adds a weak signal to the power received from the sky. The output on such hot and cold

loads is then

$$P_{\text{hot}} = K(T)(T_{\text{rec}} + fJ_{\text{hot}} + J_{\text{sky}} + g_s\eta e^{-\tau}T_A) \quad (10)$$

$$P_{\text{amb}} = K(T)(T_{\text{rec}} + fJ_{\text{amb}} + J_{\text{sky}} + g_s\eta e^{-\tau}T_A) \quad (11)$$

$$C_{\text{source}} = K(T)g_s\eta e^{-\tau}T_A \quad (12)$$

where  $f$  is a coupling coefficient between the load and the receiver. Eliminating the electronic gain  $K(T)$ .

$$K(T) = \frac{P_{\text{hot}} - P_{\text{amb}}}{f(J_{\text{hot}} - J_{\text{amb}})} \quad (13)$$

gives

$$T_A = \frac{e^{\tau}}{g_s\eta} f(J_{\text{hot}} - J_{\text{amb}}) \frac{C_{\text{source}}}{P_{\text{hot}} - P_{\text{amb}}} = T_{\text{cal}} \frac{C_{\text{source}}}{P_{\text{hot}} - P_{\text{amb}}} \quad (14)$$

The gain error is given by

$$\frac{\delta T_{\text{cal}}}{T_{\text{cal}}} = \frac{\delta T_{\text{load}} + \delta J_{\text{sky}}}{\Delta T_{\text{load}}} + 2 \frac{T_{\text{ant}}}{\Delta T_{\text{load}} \sqrt{\Delta \nu t}} \quad (15)$$

where  $\Delta T_{\text{load}} = f(J_{\text{hot}} - J_{\text{amb}})$  is the apparent load temperature difference seen from the receiver,  $\delta T_{\text{load}}$  is the typical error on the true load temperature,  $\delta J_{\text{sky}}$  the sky noise fluctuation during the measurement, and  $t$  the total time spent.

With the ALMA antennas, the coupling coefficient  $f$  to the loads in the subreflector can only be 0.8%, because of the small size of the subreflector and primary dish central hole. Thus, with the ‘‘hot’’ load at  $T_{\text{hot}} = 100^\circ\text{C}$  and the load at ambient ( $T_{\text{amb}} = 20^\circ\text{C}$ ), we have  $\Delta T_{\text{load}} = 0.64$  K only. In our attempt to get **1 % absolute calibration**, we allocate the following error budget to these three terms

1. Effective load temperature difference 0.5 %  $\Leftrightarrow \delta T_{\text{load}}/T_{\text{load}} = 0.005$
2. Noise term 0.5 %  $\Leftrightarrow 2T_{\text{ant}}/\sqrt{\Delta \nu t} = 3.2$  mK
3. Sky stability 0.7 %  $\Leftrightarrow \delta J_{\text{sky}} = 4.5$  mK

Point (1) has two contributions: the error on  $f$  and the errors (variations) on  $T_{\text{hot}}$  or  $T_{\text{amb}}$ . Equalizing these two terms requires to measure (or at least stabilize) the temperatures with  $0.2^\circ\text{C}$  accuracy, but also to determine the effective value of the coupling coefficient  $f$  to 0.35 % accuracy. This may prove extremely challenging.

The noise term (item 2) can be minimized at will, but it is important to keep in mind the typical values:

$$t = \frac{1}{\Delta \nu} \left( \frac{2 T_{\text{ant}}}{3.5 \text{ mK}} \right)^2 = 0.41 (T_{\text{ant}}/100)^2 \quad (16)$$

for 8 GHz bandwidth. While shorter than 1 second at frequencies below 300 GHz, this time rises up to 15 seconds at submm wavelengths.

The last problem in the sub-reflector load calibration is to avoid atmospheric fluctuations, which must remain below 4.5 mK. From [Lucas memo 300]

$$\delta J_{\text{sky}} = \sigma_A = \kappa(\nu)\sigma_w \left( \frac{\Delta l}{300} \right)^{0.6} \frac{1}{\sqrt{1 + (D/\Delta l)^2}} \text{ mK} \quad (17)$$

where

- $\sigma_w$  is the atmospheric path rms fluctuations of a 300 m baseline
- $\kappa(\nu)$  is the ratio of water emission to pathlength fluctuations (in mK/ $\mu\text{m}$ ) at the observing frequency. Under appropriate observing conditions,  $\kappa$  is about 20 in the submm range (see Fig.2)
- $\Delta l$  is the effective length over which the fluctuation occurs. In our case (calibration),  $\Delta l = vt/2$  where  $v$  is the tropospheric wind speed.
- the last term accounts for the averaging of  $(D/\Delta l)^2$  independent cells.

Thus, in our case,

$$\sigma_A = \kappa(\nu)\sigma_w \left(\frac{vt}{600}\right)^{0.6} \frac{1}{\sqrt{1 + (2D/(vt))^2}} \text{ mK} \quad (18)$$

with  $\sigma_w = 250\mu\text{m}$  (median pathlength fluctuation),  $v = 10$  m/s,  $D = 12$  m,  $\kappa = 10 - 20$  as appropriate for the submm frequencies,  $\sigma_A \simeq 0.08 - 0.15$  K for a cycle time of 1 second.

Temperature 0°C, Altitude 5.0 km,  $F_{\text{eff}} 0.95$ , Rejection 10 dB

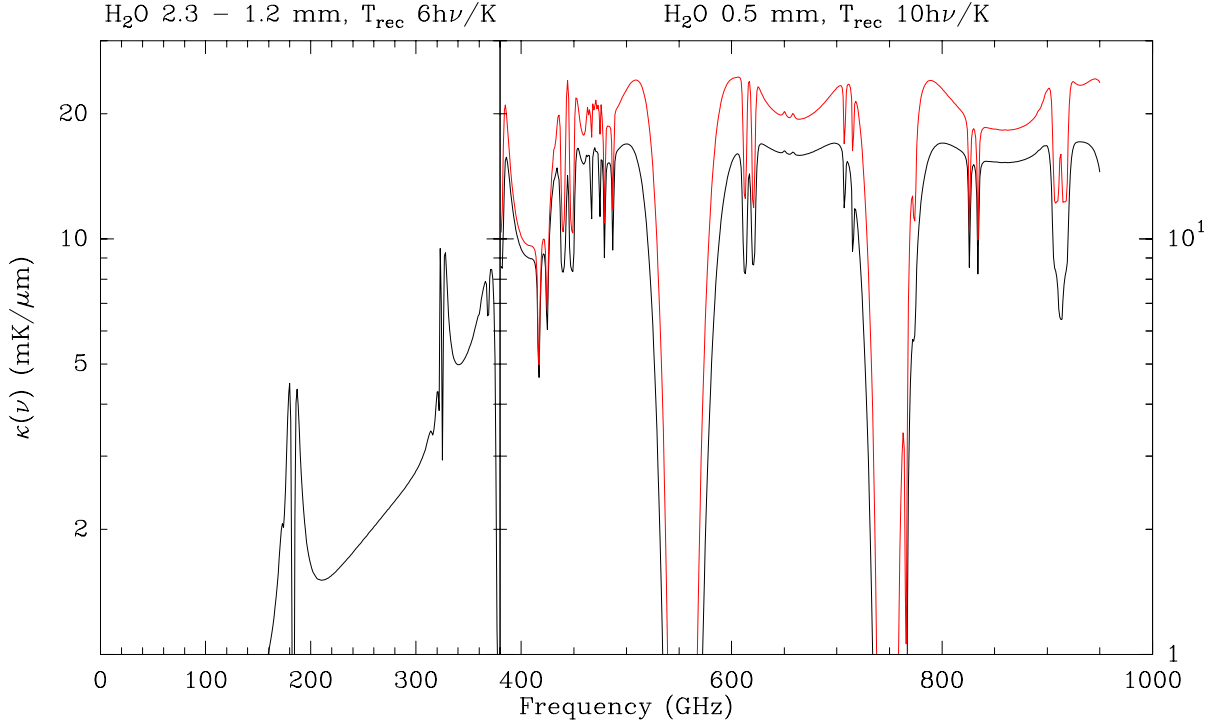


Figure 2: Relative sensitivity  $\kappa(\nu)$  of sky emissivity to pathlength fluctuations. The black curve is for typical conditions, the red curve is for optimal observing conditions (0.35 mm water vapor). Created by `default_path.astro`

We thus have to use switching times much shorter than 1 second, for which we can simplify the previous equation

$$\sigma_A = \kappa(\nu)\sigma_w(300)^{-0.6}(vt/2)^{1.6}/D \simeq 9\kappa(\nu)t^{1.6} \quad (19)$$

For  $\kappa = 20$  (best transparency at submm wavelengths), we just obtain the required 4.5 mK fluctuation level for a 10 Hz switching period. It thus seems that such a calibration device should switch at very high frequency. However, since the radiometric noise dominates, we only

need to balance the noise contributions, under the assumption that the atmospheric fluctuations get averaged as  $1/\sqrt{n}$ . Calling  $p$  the switching cycle time, and  $t$  the total integration time, we wish to have

$$\sigma_A(p, t) = \kappa(\nu)\sigma_w(300)^{-0.6}(v/2)^{1.6}/Dp^{1.6}(p/t)^{0.5} = 2\frac{T_{\text{ant}}}{\sqrt{\Delta\nu t}} = \sigma_r(t) \quad (20)$$

Or, with numerical values, taking care that  $\kappa$  is in  $\text{mK}/\mu\text{m}$ , and  $\Delta\nu = 8 \text{ GHz}$ ,

Temperature  $0^\circ\text{C}$ , Altitude 5.0 km,  $F_{\text{eff}} 0.95$ , Rejection 10 dB

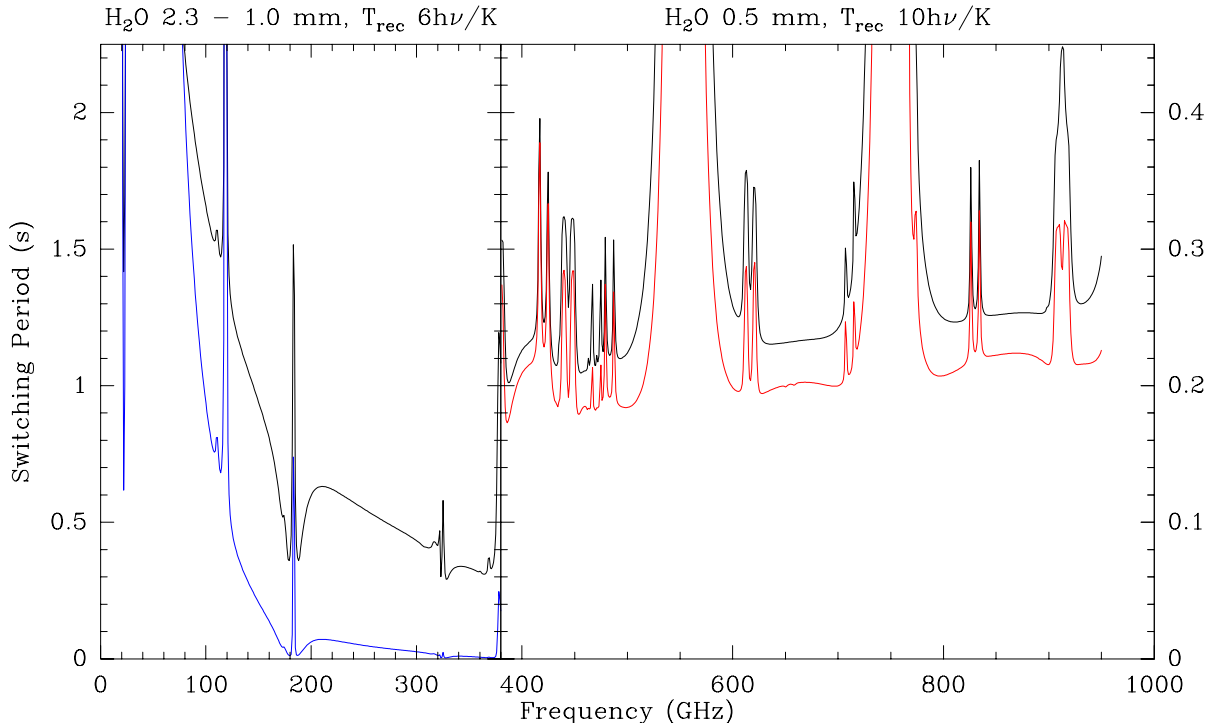


Figure 3: Maximum switching time for dual-load subreflector. The black curve is for typical conditions, the red curve is for optimal observing conditions (0.35 mm water vapor). Below 300 GHz, the switching time is limited by  $\sigma_A = 4.5 \text{ mK}$ , while above 300 GHz, it becomes limited by  $\sigma_A = \sigma_r$ . Created by `default_p.astro`

$$9\kappa(\nu)p^{2.1} = 2.2(T_{\text{ant}}/100) \quad \text{and} \quad p = \left(\frac{2.2T_{\text{ant}}/100}{9\kappa(\nu)}\right)^{\frac{1}{2.1}} \quad (21)$$

which is 0.2 seconds for nearly all frequencies above 250 GHz under typical conditions. Since in practice some margin must be left for the “good cases” (exceptional weather conditions, or better than assumed receiver performances) the calibration device **must** switch at least at 8 Hz.

This finding is surprising since the prototype tests made at BIMA provide good results even with much longer periods (up to 8 seconds). At similar frequencies (3 mm) ALMA would require periods of about 1.5 seconds. The main difference with the ALMA antennas reside in the coupling coefficient to the loads, which is about 2.2 % in the BIMA prototype. In such circumstances, at 3 mm wavelengths, the period can be much longer than 1 second, in which case we can neglect the denominator in Eq.17. The ratio of the switching periods goes then

as the ratio of the coupling coefficient to the  $\frac{1}{0.6}$  power, i.e. the BIMA system can switch 5 times slower than the system required for the ALMA antennas. Indeed, from Eq.17 for 90 GHz, where  $\kappa(\nu) \simeq 0.25$ , we obtain  $t \simeq 8$  seconds for the BIMA antennas.

## 4 Semi Transparent Vane

For the semi-transparent vane calibration method, the measurement equations are

$$\begin{aligned} P_{\text{sky}} &= K(T)(T_{\text{rec}} + J_{\text{sky}}) \\ P_{\text{load}} &= K(T)(T_{\text{rec}} + fJ_{\text{load}} + (1-f)J_{\text{sky}}) \\ C_{\text{source}} &= K(T)\eta e^{-\tau}T_A \end{aligned} \quad (22)$$

This is a one-load calibration method, for which the source antenna temperature is given by

$$T_A = fT_{\text{cal}} \frac{C_{\text{source}}}{P_{\text{load}} - P_{\text{sky}}} \quad (23)$$

where  $T_{\text{cal}}$  is the calibration temperature [Ulich & Haas, 1976]

$$\begin{aligned} T_{\text{cal}} &= J_{\text{spill}}^s - J_{\text{bg}}^s + g(J_{\text{spill}}^i - J_{\text{bg}}^i) \\ &+ (e^{\tau_s} - 1)(J_{\text{spill}}^s - J_{\text{m}}^s + g(J_{\text{spill}}^i - J_{\text{m}}^i)) \\ &+ g(e^{\tau_s - \tau_i} - 1)(J_{\text{m}}^i - J_{\text{bg}}^i) \\ &+ \frac{e^{\tau_s}}{\eta}(J_{\text{load}}^s - J_{\text{spill}}^s + g(J_{\text{load}}^i - J_{\text{spill}}^i)) \end{aligned} \quad (24)$$

This expression has two useful limiting cases: the homogeneous temperature case  $J_{\text{load}} \simeq J_{\text{m}} \simeq J_{\text{spill}}$  for which

$$T_{\text{cal}} \simeq (1+g)J_{\text{m}} \quad (25)$$

and the low opacity case  $\tau \ll 1$ , for which

$$T_{\text{cal}} \simeq \frac{1+g}{\eta}(J_{\text{load}} - (1-\eta)J_{\text{spill}}) \quad (26)$$

Neglecting the measurement noise, a 1% gain precision requires that  $K(T)$  varies less than 1% between the load and sky measurement. From Eq.22, in the semi-transparent vane calibration system, this variation is

$$\Delta K = K(f(J_{\text{load}} - J_{\text{sky}}) + T_{\text{ant}}) - K(T_{\text{ant}}) \quad (27)$$

which we want to be less than some fraction  $y$ , i.e. using Eq.7,

$$f(J_{\text{load}} - J_{\text{sky}}) \leq y(T_{\text{sat}} + T_{\text{ant}}) \quad (28)$$

which gives

$$f \leq y \frac{T_{\text{sat}} + T_{\text{ant}}}{J_{\text{load}} - J_{\text{sky}}} \quad (29)$$

In practice, only loads at the ambient temperature can have an accurately defined effective temperature  $J_{\text{load}}$ , for which a 0.2°C temperature error result in 0.07 % uncertainty. Loads at other temperatures must be insulated to avoid temperature gradients at the load surface, but

such an insulation requires an infrared shield. The uncertainty in the reflection coefficient of this insulation layer at mm or submm wavelengths could dominate the calibration accuracy. It is clear from Eq.29 that the biggest problem, i.e. the lowest values of  $f$ , occur at the longest wavelengths, because the lower values of  $T_{\text{sat}}$  (see Eq.7-8),  $T_{\text{ant}}$  and  $J_{\text{sky}}$  concur to minimize the allowed value of  $f$ .

Limiting the saturation to  $y = 0.8\%$ , the values of  $f$  as function of frequency and saturation temperature  $T_{\text{sat}}$  are displayed in Fig.4. Clearly, the vane is only required at frequencies below

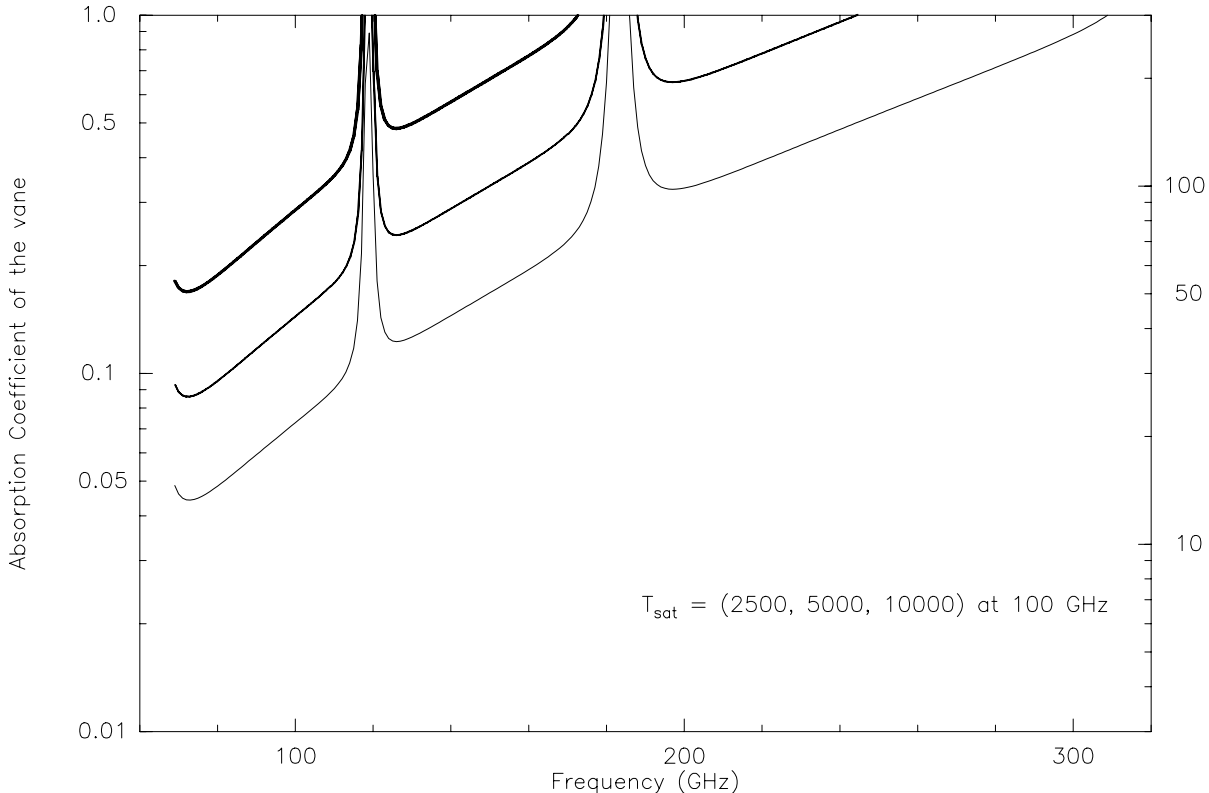


Figure 4: Vane absorption coefficient  $f$  as a function for frequency. The three curves, from thin to thick, are for  $T_{\text{sat}} = 2500, 5000$  and  $10000$  K at  $100$  GHz. The right axis indicate the effective load temperature (K).

$300$  GHz. Above that, the normal ambient load can be used. We can neglect the noise on the measurement, since the integration time required to get  $0.5\%$  accuracy is given by

$$\frac{2 T_{\text{ant}}}{\sqrt{\Delta\nu t}} = 0.5f(J_{\text{load}} - J_{\text{sky}}) \simeq 0.5yT_{\text{sat}} \quad (30)$$

$$t \simeq \frac{4}{\Delta\nu} \left( \frac{T_{\text{ant}}}{yT_{\text{sat}}} \right)^2 \quad (31)$$

which is much less than  $1$  s, in all circumstances.

A big advantage of the semi-transparent vane calibration system reside in the possibility to accurately calibrate the absorption coefficient  $f$  by observing a source with or without the vane in front of the receiver. Since we have allowed  $y = 0.8\%$  for the saturation,  $f$  must be measured with  $0.5\%$  accuracy to remain consistent with our goal of  $1\%$  total error. The integration time required to do so is an interesting parameter, because if it is short enough,

it is possible to have the vane moved by a (relatively) slow and simple system. If not, the vane must be mounted on some chopping system to provide periods of order 1 sec. This is to guarantee stable statistical properties of the atmospheric conditions between the on-vane and off-vane observations, both in transmission and phase noise.

To estimate this integration time, we use the antenna-based noise equivalent flux  $S_0$  as derived by [Moreno & Guilloteau, memo 372], and consider that we can move to a source of flux  $S$  to perform this measurement. Let  $x = 1 - f$  be the transmission coefficient of the vane. The vane-on signal is  $xS$ , while the vane-off signal is  $S$ . To equalize the error terms on the ratio of the two measurements,  $S$  and  $xS$ , we need to spend  $t_{\text{on}} = t/(1 + x^2)$  with the vane on, and only  $t_{\text{off}} = tx^2/(1 + x^2)$  with the vane off for a total time  $t$ , and the resulting error is

$$\frac{\delta x}{x} = \frac{2\sqrt{1+x^2}S_0}{Sx\sqrt{t\Delta\nu}} \quad (32)$$

which, when converted to  $f$ , results in

$$\frac{\delta f}{f} = \frac{2\sqrt{1+(1-f)^2}S_0}{Sf\sqrt{t\Delta\nu}} \quad (33)$$

Figure 5 gives the resulting integration time as function of frequency. The calibration source is a quasar of 1.5 Jy, and spectral index  $-0.7$ , which can be found within 5 degrees of any source. Three cases are considered: an absorption coefficient fixed to the value required by 90 GHz observations (plain curves), an absorption coefficient maximized for each frequency (long dashed curves). The last case (short dashed curves) correspond to “normal” lossy material will have an absorption coefficient proportional to the frequency (scaled to the required value at 90 GHz). Fig.5 indicates that the time required at 90 GHz is of order of 5–10 minutes, with about 10 % of the time spent vane off, i.e.  $\simeq 30$  s, and 90 % vane on. These long times occur because the useful signal is actually  $\min(fS, (1-f)S)$  instead of  $S$  as assumed by [Plambeck memo 321].

An additional problem which must be worked out is the possible different decorrelation factors on the vane-on and vane-off measurement, due to the different integration times. For long timescales, there is actually a component of the WVR correction which depends on the initial error, due to the limited accuracy of the prediction. Assuming a 10% accuracy for the correction, an estimate to this residual error is given by

$$\Delta P = 0.1\sigma_w (\min(B, vt)/300)^{0.6} \mu\text{m} \quad (34)$$

where  $t$  is the timescale,  $v$  the wind speed, and  $B$  the typical baseline length. Since  $B < vt$  and  $B \leq 1$  km except on the largest configuration (where the outer scale of the atmosphere would limit anyhow), we obtain  $\Delta P \leq 25\mu\text{m}$ , for which the decorrelation is 2.5 % at 300 GHz, but below 1 % at frequencies below 230 GHz. Hence, variable decorrelation should not be a severe issue.

Even taking into account the natural increase of the absorption coefficient with frequencies, the time required to measure  $f$  becomes quite long (15–30 minutes) at the highest frequencies. This indicates that using a second vane, with higher absorption coefficient  $f$ , could be useful. With two vanes, the best boundary frequency is near 160 GHz, with the second vane having an absorption coefficient 1.7 times that of the first vane (the exact values obviously depend on the saturation values of the various receivers). The integration time required to calibrate the vane coefficient stays then below  $\sim 15$  minutes at all frequencies. Above 300 GHz, a normal ambient load should be used. Note however that keeping the saturation temperature higher than  $5000(\nu/100 \text{ GHz})^2$  would help considerably.

Temperature 0°C, Altitude 5.0 km,  $F_{\text{eff}}$  0.95, Rejection 10 dB

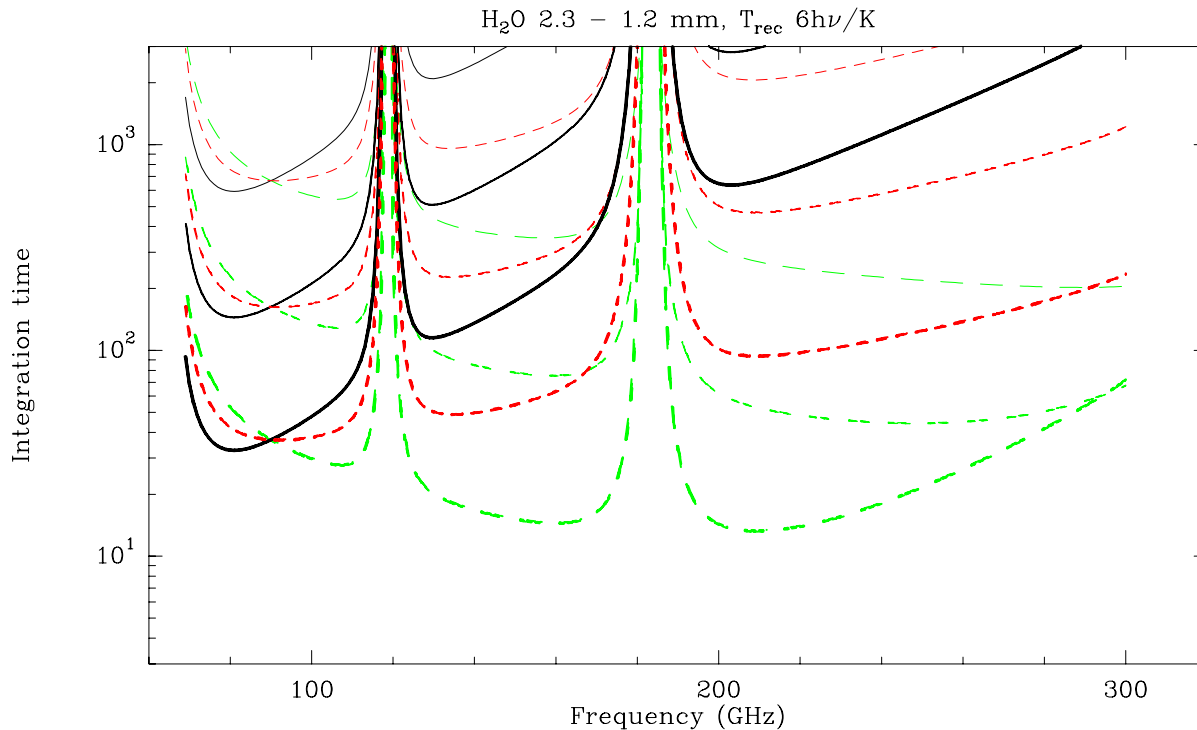


Figure 5: Integration time to measure the absorption coefficient  $f$  with 0.5 % accuracy on a typical quasar. The three curves, from thin to thick, are for  $T_{\text{sat}}$  ranging from 2500, 5000 and 10000 K at 100 GHz, respectively. Plain curves for  $f$  set to the value required at 90 GHz, long dashed curves are for optimized absorption coefficient  $f$  as function of frequency, short dashed curves for typical lossy material ( $f \propto \nu$ ).

Since the absorption coefficient calibration time is significant, we conclude that the commutation system should have a settling time of order 1 sec or less.

## 5 Conclusions

Table 2 summarizes the pro and cons of the two approaches. The vane approach clearly offers a number of advantages, in terms of speed, calibration, and maintenance facility. It is thus urgent to develop a prototype of the vane system

Our work offers the basic for such a study. Two vanes, the first one with an absorption coefficient of  $0.06(\nu/100\text{GHz})$  below 160 GHz, the second one of  $0.12(\nu/100\text{GHz})$  between 160 and 300 GHz, seem sufficient to satisfy the requirements. In addition to the semi-transparent vanes, a standard absorber should be provided for frequencies above 300 GHz.

A possible temptation would be to discard SIS mixers for band 3 at the benefit of HEMT amplifiers, which have much less saturation problems. This would only be acceptable if the noise performances remain within the specifications, both in noise ( $< 6h\nu/k + 4\text{ K}$ , measured in front of the receiver package) and stability ( $\sim 10^{-4}$ ). Moreover, this would only solve the Band 3 problem: a semi-transparent vane would still be required for Band 4,5 and 6.

Finally, one should mention that some astronomical sources will actually be strong enough to produce some receiver saturation. The Sun is one obvious case, but calibration accuracy is

	Vane system	Dual-load
Location	<b>In receiver cabin</b>	<i>In subreflector</i>
Thermal control	<b>At ambient, need measurement only</b>	<i>Need heating system at 100° C in subreflector</i>
Speed	<b>Slow device (1-2 sec)</b>	<i>Fast switching (10 Hz)</i>
Reliability	<b>Simple device</b>	<i>Possible sealing problems at subreflector interface</i>
Maintenance	<b>Easy access</b>	<i>Awkward location</i>
Integration time	<b>Short (&lt; 1 sec)</b>	<i>Up to 5 sec at submm frequencies</i>
Basic Calibration	<b>In a few minutes, on sky</b>	<i>Not demonstrated</i>
Development	<i>to be done</i>	<b>Prototype working</b>

Table 2: Pro and Con of the vane and dual-load calibration systems. **Pros** are in **boldface**, while *Cons* are in *italics*.

unlikely to be real issue in this case. Jupiter and Venus are also too bright and will lead to some saturation. This is not a critical issue for imaging these objects, but prevent their use as primary calibrators. Fortunately, among the possible primary flux calibrators such as Mars and Uranus, Mars only gets too bright at its most favorable oppositions (a couple of weeks every 14 years) for the lowest saturation temperature  $T_{\text{sat}} = 2500$  K, while Uranus is always weak enough.

## References

[Lucas memo 300]

Lucas, R. (2000)  
Reducing Atmospheric noise in single-dish observations with ALMA. *ALMA Memo 300*.

[Mangum memo 318]

Mangum, J. 2000  
Amplitude Calibration at Millimeter and Sub-millimeter Wavelengths *ALMA memo 318*

[Plambeck memo 321]

Plambeck, R., 2000  
Receiver Amplitude Calibration for ALMA *ALMA memo 321*

[Bock et al. memo 225]

Bock, D., Welch, W.J., Fleming, M. & Thornton D., 1998  
Radiometric Calibration at the Cassegrain Secondary Mirror *ALMA memo 225*

[Tucker & Feldman 1985]

Tucker, J.R, Feldman, M.J. 1985

Quantum Detection at Millimeter Wavelengths  
Review of Modern Physics, 57, 1055-1113

[Ulich & Haas, 1976]

Ulich, R. & Haas, R.W., 1976

Amplitude Calibration of Millimeter Wavelengths Spectral Lines

ApJ Supp. 30, 247

[Moreno & Guilloteau, memo 372]

Moreno, R., & Guilloteau, S. 2000,

ALMA Calibration: Requirements on the integration times, and suggested observing strategies.

*ALMA memo 372, in prep.*